Photoinduced high-Chern-number quantum anomalous Hall effect from higher-order topological insulators

Xiaolin Wan,[1] Zhen Ning,[1] Dong-Hui Xu,[1,2,*] Rui Wang,[1,2] and Baobing Zheng[3,1,†]

[1]*Institute for Structure and Function & Department of Physics & Chongqing Key Laboratory for Strongly Coupled Physics, Chongqing University, Chongqing 400044, People's Republic of China*

[2]*Center of Quantum Materials and Devices, Chongqing University, Chongqing 400044, People's Republic of China*

[3]*College of Physics and Optoelectronic Technology, Baoji University of Arts and Sciences, Baoji 721016, People's Republic of China*

(Received 18 July 2023; accepted 13 February 2024; published 29 February 2024)

Quantum anomalous Hall (QAH) insulators with high Chern number host multiple dissipationless chiral edge channels, which are of fundamental interest and promising for applications in spintronics and quantum computing. Here, we propose a dynamic approach for achieving high-Chern-number QAH phases in periodically driven two-dimensional higher-order topological insulators (HOTIs) irradiated by circularly polarized light (CPL). In particular, we consider two representative kinds of HOTIs which are characterized by a quantized quadruple moment and the second Stiefel-Whitney number, respectively. Using the Floquet formalism for periodically driven systems, we demonstrate that QAH insulators with tunable Chern numbers up to four can be achieved. Moreover, we show by first-principles calculations that the monolayer graphdiyne, a realistic HOTI, is an ideal material candidate. Remarkably, the irradiation of CPL does not destroy the quantized quadruple moment in periodically driven HOTIs, leading to an exotic mixed phase harboring both high Chern numbers and higher-order topology. Our work not only establishes a strategy for designing high-Chern-number QAH insulators in periodically driven HOTIs, but also provides a powerful approach to investigate exotic topological states in nonequilibrium cases.

DOI: 10.1103/PhysRevB.109.085148

I. INTRODUCTION

The quantum anomalous Hall (QAH) effect, characterized by quantized Hall resistance in the absence of external magnetic field, exhibits nontrivial chiral edge states that conduct dissipationless charge current. This intriguing property facilitates its potential applications for low-power consumption electronic devices, thus drawing considerable attention [1–5]. The Chern number $\mathcal{C}$, also known as the TKNN number and defined by the integration of the Berry curvature over the first Brillouin zone (BZ) [6], denotes the number of topologically protected chiral edge states, and the Hall resistance of a QAH insulator is quantized into $h/\mathcal{C}e^2$, where h is the Planck's constant and e denotes the charge of an electron. Usually, the QAH state with $\mathcal{C} = 1$ has been widely studied both in theories and experiments [7–12]. The low-Chern-number QAH phase (i.e., $\mathcal{C} = 1$), which possesses a single current transport channel, may encounter challenging issues in practical applications due to unavoidable contact resistance restrictions [9,13,14]. In contrast, the high-Chern-number QAH states (i.e., $\mathcal{C} > 1$) provide more topologically protected chiral edge channels, which can significantly improve the performance of QAH-based devices. More importantly, the high-Chern-number QAH insulators can enhance the effective breakdown current of edge states and thus provide an efficient solution to the contact resistance problem [9,13,14]. However, to date, only a limited number of high-Chern-number QAH insulators have been reported in magnetically doped or intrinsic magnetic topological insulator (TI) films [13–22].

The QAH effect is generally suggested to be achieved in two-dimensional (2D) topological insulators (TIs) by breaking time-reversal ($\mathcal{T}$) symmetry [23–29], and consequently the $\mathcal{T}$-broken band topology indicates that chiral edge states are a necessary feature of the one-dimensional boundaries in two spatial dimensions, as dictated by the bulk-boundary correspondence. Recently, the guiding principle for TIs has been extended to higher-order topological insulators (HOTIs), which manifest that the dimensionality of topologically gapless boundary states is lower by more than one dimension compared to that of the bulk [30–34]. The novel bulk-boundary correspondence has propelled HOTIs into the forefront of research in the field of topological phases of matter [32–46]. The $\mathcal{T}$ symmetry plays a vital role in protecting the higher-order boundary states in HOTIs associated by the crystalline symmetries [32–34], even though crystalline symmetries are not essential [33,47,48]. Therefore, in light of the fundamental expansion of topological states of matter, it is imperative to investigate topological phase transitions by introducing $\mathcal{T}$-symmetry breaking in HOTIs. To be specific, there are currently at least two unresolved issues about this problem: (i) the connection between the QAH and high-Chern-number QAH states and the $\mathcal{T}$-broken HOTIs; (ii) the realization approach and material candidate, if issue (i) is established.

*donghuixu@cqu.edu.cn
†scu_zheng@163.com

Motivated by the above issues, we here propose a strategy for achieving the high-Chern-number QAH insulators from 2D $\mathcal{T}$-invariant HOTIs irradiated by circularly polarized light (CPL). We focus on two representative types of 2D HOTIs whose bulk topology can be respectively measured by a quantized quadruple moment [30,31] and the second Stiefel-Whitney number [49]. Within the framework of the Floquet formalism, their results show a surprise common sense; that is, the high-Chern-number QAH phase is derived from the light-induced multiple band inversion collaborated by higher-order band topology, which is different from the high-Chern-number QAH phase arising from the trigonal warping effect in the previous work [50]. In particular, the latter one has been realized in 2D graphdiyne [41,51]. It is noteworthy that, besides the application of external magnetic fields and magnetic dopant atoms, the utilization of periodically driven light fields is considered to be an effective approach for breaking $\mathcal{T}$ symmetry and exploring exotic topological phases out of equilibrium [8,52–59]. The Chern number is continuously tunable from one to four by changing the light intensity and photon energy. Intriguingly, we further reveal that the irradiation of CPL does not destroy the quantized quadruple moment, and the unique Floquet topological state harboring both high Chern numbers and higher-order topology offers a promising avenue to investigate exotic topological states in nonequilibrium cases.

II. HIGH-CHERN-NUMBER QAH STATE FROM THE QUADRUPLE INSULATOR

We start with the Benalcazar-Bernevig-Hughes (BBH) Hamiltonian for a quantized quadrupole insulator described as [30,31]

$$H(\mathbf{k}) = \lambda \sin(k_y)\Gamma_1 + [\gamma_y + \lambda\cos(k_y)]\Gamma_2 + \lambda \sin(k_x)\Gamma_3 + [\gamma_x + \lambda\cos(k_x)]\Gamma_4, \quad (1)$$

in which $\mathbf{k} = (k_x, k_y)$ is the wave vector, λ and γ represent two kinds of hopping strengths, $\Gamma_i = -\tau_2\sigma_i$ ($i = 1, 2$, and 3), and $\Gamma_4 = \tau_1\sigma_0$ (here, τ and σ denote two sets of Pauli matrices for different degrees of freedom). For simplicity and without loss of generality, we hereafter assume $\lambda = 1$ and $\gamma_x = \gamma_y = \gamma$. It is worth noting that bands near the Fermi level are located at (π, π) or (0, 0) when $\lambda/\gamma > 0$ or $\lambda/\gamma < 0$. However, the topological condition for the quadrupole insulator only depends on the absolute value of the ratio of λ and γ. Here, we choose the $\lambda/\gamma < 0$ and mainly focus on the topological properties at the $\Gamma = (0, 0)$, and expand Eq. (1) to the k-quadratic order around Γ to obtain the low-energy effective model $H(\mathbf{k}) = k_y\Gamma_1 + M_y\Gamma_2 + k_x\Gamma_3 + M_x\Gamma_4$, where $M_{x(y)} = 1 + \gamma - \frac{1}{2}k^2_{x(y)}$. To study the influence of light field on the quadrupole insulator, we apply a time-periodic and spatially homogeneous CPL that can be described by vector potential of $\mathbf{A}(t) = A[\cos(\omega t), \eta\sin(\omega t), 0]$ for polarization in the x-y plane, in which A is the amplitude, $\omega = 2\pi/T$ is frequency of light, and $\eta = \pm$ are for right- and left-handed CPL that rotates counterclockwise and clockwise in the x-y plane, respectively. The coupling of the time-periodic CPL on the effective Hamiltonian can be described by Peierls substitution, resulting in time-dependent Hamiltonian $H(\mathbf{k}, t) = H(\mathbf{k} + \frac{e}{\hbar}\mathbf{A}(\mathbf{t}))$ [60,61]. Then, we expand the CPL driven Hamiltonian by discrete Fourier series and obtain $H(\mathbf{k}, t) = \sum_m H_m(\mathbf{k})e^{-im\omega t}$. The Fourier components $H_m(\mathbf{k})$ read

$$H_m(\mathbf{k}) = \frac{1}{T}\int_0^T e^{im\omega t}H(\mathbf{k} + \frac{e}{\hbar}A(t))dt. \quad (2)$$

Based on Eq. (2), we can construct an effective static Hamiltonian $H(\mathbf{k}, \omega)$ in the infinite extended Hilbert space of multiphoton components [see details in the Supplemental Material (SM)] [61–63]. After careful inspection of the convergence of the Floquet quasienergy spectrum, we find that the first-order truncation is accurate enough to describe the irradiation of CPL (see Fig. S2 in the SM [63]), and the higher-order terms that correspond to the contributions of two-photon and beyond have negligible influence on the Floquet quasienergy spectrum. Therefore, we here truncate the infinite Floquet bands to first order in the following discussion. The considered terms read,

$$\begin{aligned} H_0(\mathbf{k}) &= k_y\Gamma_1 + (M_y - B^2)\Gamma_2 + k_x\Gamma_3 + (M_x - B^2)\Gamma_4 \\ H_{\pm1}(\mathbf{k}) &= B[\Gamma_3 - k_x\Gamma_4 \pm i(\Gamma_1 - k_y\Gamma_2)\eta] \\ H_{\pm2}(\mathbf{k}) &= \frac{B^2}{2}(\Gamma_2 - \Gamma_4), \end{aligned} \quad (3)$$

where $B = \frac{Ae}{2\hbar}$. By diagonalizing the truncated Floquet Hamiltonian $H(\mathbf{k}, \omega)$ in the momentum and frequency space, we can obtain Floquet quasienergy bands of the quadrupole insulator around Γ under irradiation of CPL. We here mainly present the effect of left-handed CPL on the quadrupole insulator and will no longer show the case of right-handed CPL any more because it has an equivalent effect on the quadrupole insulator as that of left-handed CPL. As is well known, our employed BBH model exhibits a trivial quadrupole phase without gapless edge states for $|\gamma/\lambda| > 1$, while a nontrivial quadrupole phase with quantized corner states for $|\gamma/\lambda| < 1$. Therefore, we have set $|\gamma/\lambda| = 0.9$ to guarantee that the CPL is incorporated into the nontrivial quadrupole phase.

The calculated Floquet quasienergy bands with increasing light intensity $eA/\hbar$ and and photon energy $\hbar\omega$ are shown in Fig. 1. In the absence of irradiation of CPL, the energy spectrum characterizes with a direct band gap between the conduction band minimum (CBM) and the valence band maximum (VBM) at Γ, and exhibits corner zero modes as expected [31]. When the CPL is introduced, the originally well-separated CBM and VBM respectively move downward and upward, leading to the closing and reopening of band gap, forming the inverted bands. As shown in Fig. 1(a) (with light intensity $eA/\hbar = 0.03$ Å^{-1} and photon energy $\hbar\omega = 0.13$ eV), the Floquet quasienergy bands still keep a trivial insulating state because of the relatively small photon energy. As we increase the photon energy ($\hbar\omega = 0.14$ eV), one can evidently see the band inversion emerges between the Floquet-Bloch bands near the Fermi level (i.e., C_{-1} and V_1), shown in Fig. 1(b). To characterize the topological property, we can calculate the Chern number $\mathcal{C}$ of the Floquet system, which can be given by an integral of the Berry curvature of the occupied bands [64]. The calculated Chern number $\mathcal{C} = 1$ further

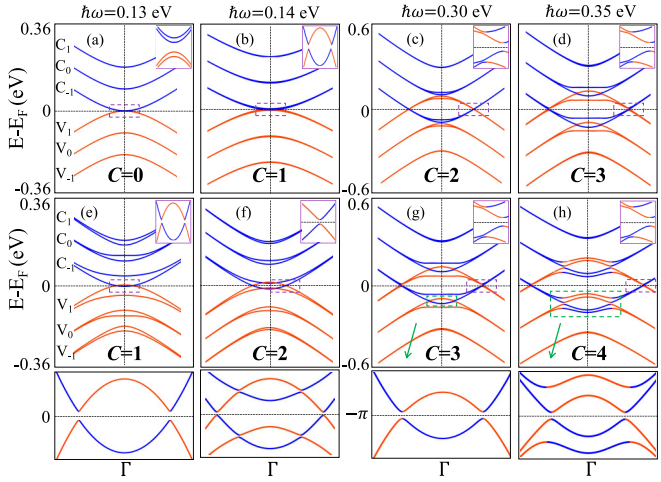

FIG. 1. The evolution of energy spectrum of quadrupole insulator under irradiation of CPL with the increasing light intensity $eA/\hbar$ and photon energy $\hbar\omega$, in which the corresponding calculated Chern number are marked, $C_{1,0,-1}$ and $V_{1,0,-1}$ represent the photon-dressed bands near the Fermi level, respectively. In (a)–(d), the light intensity $eA/\hbar$ is set to 0.03 Å^{-1}, while $eA/\hbar = 0.08$ Å^{-1} in (e)–(h). The photon energy of CPL in the same vertical column, as labeled on the top of corresponding columns, are 0.13, 0.14, 0.30, and 0.35 eV, respectively. The insets enlarge the bands in the dashed box near the Fermi level. Here, we have set $|\gamma/\lambda| = 0.9$ for all the calculations to guarantee the nontrivial quadrupole phase of the BBH model.

confirms the nontrivial band topology, and demonstrates that the nontrivial quadrupole insulator evolves into a quantum anomalous Hall (QAH) insulator under irradiation of CPL.

More importantly, continuous increase in photon energy drives further evolution of the photon-dressed band structure and induces multiple band inversion for the quadrupole insulator. As shown in Figs. 1(c) and 1(d), the inversion of Floquet-Bloch bands appears two and three times, characteristic of higher Chern number $\mathcal{C} = 2$ and $\mathcal{C} = 3$, respectively. That is to say, under the irradiation of CPL, we can obtain the high-Chern-number QAH states from a quadrupole insulator, and the Chern number can be continuously manipulated by changing the photon energy. Meanwhile, by tuning the light intensity at the given photon energy, the Chern number of the Floquet system can be also continuously changed. For example, at certain photon energy $\hbar\omega = 0.14$ eV, the corresponding Chern number changes continuously from one to two as the light intensity increases from 0.03 Å^{-1} to 0.08 Å^{-1} [compare Fig. 1(b) with Fig. 1(f)]. The maximum Chern number of the Floquet system that we can obtain is four, as shown in Fig. 1(h) with $eA/\hbar = 0.08$ Å^{-1} and $\hbar\omega = 0.35$ eV. Besides, it is worth noting that the chiral edge states may not be uniquely determined by the Chern number $\mathcal{C}$ in periodically driven 2D systems [57–59]. However, as shown in the bottom panels of Fig. 1, with increasing frequency, band inversions occur first at $\varepsilon = 0$, then at $\varepsilon = \pi$, leading to high Chern number phases. Hence, in our work, the Chern number $\mathcal{C}$ calculated from the Floquet bands below the Fermi level can enough determine the possible number of chiral edge states. In short, utilizing the BBH model and Floquet theory, we demonstrate that the 2D quadrupole insulator evolves into

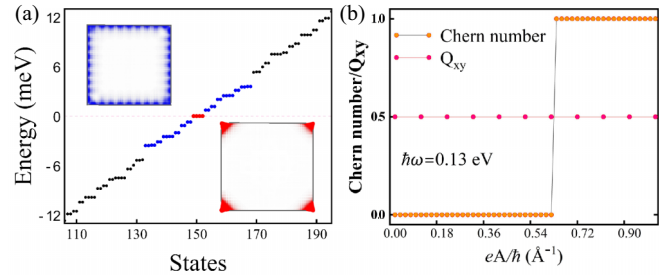

FIG. 2. (a) The energy spectrum with open boundaries in both the x and y directions, where the edge states and corner states are marked in blue and red, respectively. The spatial distribution of the corner and edge states are shown as the inserts. (b) The evolution of Chern number $\mathcal{C}$ and quadruple moment Q_{xy} with the increase of light intensity.

the Floquet QAH insulator with tunable high Chern numbers under the irradiation of CPL.

To better understand the above promising phenomenon from the quadrupole insulator to high-Chern-number QAH states, we further determine whether the higher-order topology is preserved under the irradiation of CPL. To reveal this, we calculate the energy spectrum by directly diagonalizing the Floquet Hamiltonian Eq. (3) with open boundaries in both the x and y directions, as show in Fig. 2(a). It is found that both 1D edge states (colored blue) and 0D corner states (colored red) inside the gap, indicating the coexistence of quadrupole insulator and Chern insulator phases. As confirmed in Fig. 2(b), the quadruple moment Q_{xy} can always be quantized to 1/2 with the increase of light intensity, indicating that the irradiation of CPL does not destroy the higher-order topology; meanwhile, the Chern number $\mathcal{C}$ accompanies with a transition from zero to one. Further, we also find the phase with $\mathcal{C} = 2$ or $\mathcal{C} = 3$ and $Q_{xy} = 1/2$ are present at higher frequencies (see Fig. S2 in the SM [63]). The discovery that CPL triggers a phase transition to high-Chern-number QAH insulators from HOTIs not only establishes periodically driven HOTIs as a practical platform for achieving high Chern number QAHE, but also unveils a unique Floquet topological state harboring both high Chern numbers and higher-order topology.

III. HIGH-CHERN-NUMBER QAH STATE FROM A HOTI WITH SECOND STIEFEL-WHITNEY NUMBER AND ITS REALIZATION IN GRAPHDIYNE

Next, we show that the photoinduced high-Chern-number QAH states can also occur in a HOTI with the second Stiefel-Whitney number. This type of HOTIs was realized in 2D graphdiyne [41,51], whose bulk topology can be revealed by a four-band $k \cdot p$ Hamiltonian as [41,65]

$$H = \left(-\Delta + mk_x^2 + mk_y^2\right)\sigma_z\tau_0 + vk_x\sigma_x\tau_x + vk_y\sigma_x\tau_y + \lambda\left(k_x^2 - k_y^2\right)\sigma_z\tau_x + 2\lambda k_x k_y\sigma_z\tau_y. \quad (4)$$

The calculation details and related results are included in the SM [63]. As shown in Fig. S1 [63], we can see that multiple band inversion of Floquet bands emerges and the 2D HOTI with the second Stiefel-Whitney number evolves into the Floquet QAH insulator with tunable Chern number

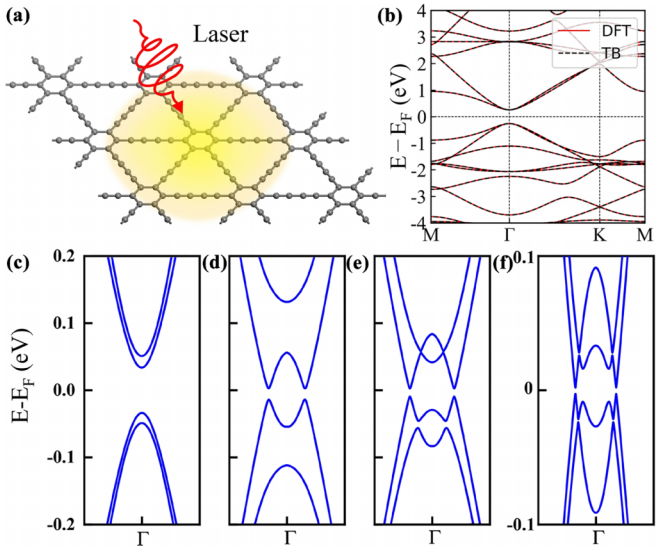

FIG. 3. (a) Schematic of irradition of CPL on graphdiyne. (b) The band structures of graphdiyne obtained by DFT calculation (red solid lines) and Wannier TB Hamiltonian (black dashed lines) without irradition of CPL. (c)–(f) The Floquet band structures of graphdiyne around Γ under irradition of CPL with different light intensity $eA/\hbar$ and photon energy $\hbar\omega$. In (c), with the parameters $eA/\hbar = 0.01$ Å^{-1} and $\hbar\omega = 0.2$ eV, the Floquet bands are trivial; In (d), the Floquet bands with $eA/\hbar = 0.04$ Å^{-1} and $\hbar\omega = 0.2$ eV exhibit band inversion with $\mathcal{C} = 1$ near the Fermi level; In (e), the Floquet bands with $eA/\hbar = 0.03$ Å^{-1} and $\hbar\omega = 0.31$ eV evolve into the high-Chern-number states with $\mathcal{C} = 2$; With the parameters $eA/\hbar = 0.02$ Å^{-1} and $\hbar\omega = 0.4$ eV in (f), the Chern number of the Floquet system increases to three.

under the irradiation of CPL, which is quite similar to the results obtained from the quadrupole insulator described by BBH model.

The material realization will greatly facilitate the potential applications of photoinduced QAH states from 2D HOTIs. Considering that 2D graphdiyne was experimentally synthesized [66], by employing first-principles calculations and a tight-binding (TB) model combined with Floquet theory, we next take it as an example to confirm the photoinduced topological phase transition from the HOTI to high-Chern-number QAH states in 2D graphdiyne. Due to the negligible spin-orbital coupling of graphdiyne, we treat it as a spinless system in the following discussions. For first-principles calculations we adopted the Perdew-Burke-Ernzerhof exchange-correlation functional within the framework of density functional theory (DFT) as implemented in the Vienna *ab initio* simulation package [67–69]. The other calculated details can be found in the SM [63]. Figure 3(a) shows the optimized crystal structure of graphdiyne constructed from *sp*- and sp^2-hybridized carbon atoms. The calculated lattice constant is 9.46 Å, which shows excellent consistency with previous experimental and theoretical results [41,70,71]. The obtained band structure, as illustrated in Fig. 3(b), shows that it possesses a direct band gap of 0.47 eV at Γ, which agrees well with the previous theoretical result of 0.46 eV [72].

Based on the obtained band structure, we established a real-space Wannier TB Hamiltonian for graphdiyne. Note that, in order to ensure the accuracy and reliability of our following analysis, the band structures calculated by the TB Hamiltonian should be in good agreement with those computed by first-principle calculations, shown in Fig. 3(b). Employing the Floquet theorem, we can introduce the CPL in the real-space TB Hamiltonian in the Wannier function basis and obtain an effective static Hamiltonian $H(\mathbf{k}, \omega)$ in the frequency and momentum space. The further details for $H(\mathbf{k}, \omega)$ can be found in the SM [63].

According to the truncated $H(\mathbf{k}, \omega)$, we computed the band structure of 2D HOTI graphdiyne under the irradiation of CPL as implemented in WannierTools code [74]. The calculated band structures around Γ under various light intensity and photon energy of CPL are shown in Figs. 3(c)–3(f). Evidently, the bands around Γ can be inverted by tuning the light intensity and photon energy. Similar to the case of the BBH model, the multiple band inversion occurs as expected, leading to the Chern number manipulated continuously from trivial state $\mathcal{C} = 0$ to nontrivial QAH state with $\mathcal{C} = 3$. It is worthwhile to mention the higher Chern number larger than three can also be realized in graphdiyne by further tuning light intensity and photon energy.

To demonstrate the topological properties of the photoinduced QAH states, we next show the hallmark of the QAH phases with tunable Chern number by depicting their edge states. Figure 4(a) illustrates the edge states of graphdiyne under the irradiation of CPL along zigzag direction $-\overline{\mathrm{X}} \leftarrow \overline{\Gamma} \rightarrow \overline{\mathrm{X}}$. One can see that the number of the chiral edge states with different light intensity and photon energy show good agreement with the DFT band calculations, further supporting the fact that we can obtain the QAH states by irradiating CPL on a 2D HOTI. Moreover, by manipulating the light intensity and photon energy, we can realize the high-Chern-number QAH states up to $\mathcal{C} = 4$ for graphdiyne. Here, it is clearly found that the calculated Chern number $\mathcal{C}$ uniquely corresponds to the number of chiral edge modes inside the band gap, demonstrating the reliability of our calculation. Considering graphdiyne as a 2D realistic HOTI, it is the first HOTI platform to achieve the high-Chern-number QAH states under the irradiation of CPL. In addition, the maximum light intensity $eA/\hbar = 0.07$ Å^{-1} in Fig. 4 corresponds to the electric field strength of 3.50×10^9 V/m or the laser energy density 1.62×10^{11} W/cm^2. Hence, the laser frequencies and intensities we used in our calculations are entirely feasible to replicate in experimental settings [8,73].

The phase diagram can completely summarize the parameter regimes of different phases and gain a deep insight into the topological phase transition. Therefore, based on the $H(\mathbf{k}, \omega)$ obtained from first-principles calculations, we obtain the phase diagram of Chern number for graphdiyne as a function of light intensity and photon energy of CPL, as shown in Fig. 4(b). We can find that there are five distinct phase regimes corresponding to the continuously changed Chern number (ranging from zero to four). With relatively small light intensity and photon energy, the Chern number increases from zero to four with the increasing light intensity and photon energy. However, when the light intensity and photon energy is relatively high, it is found that further increase of light

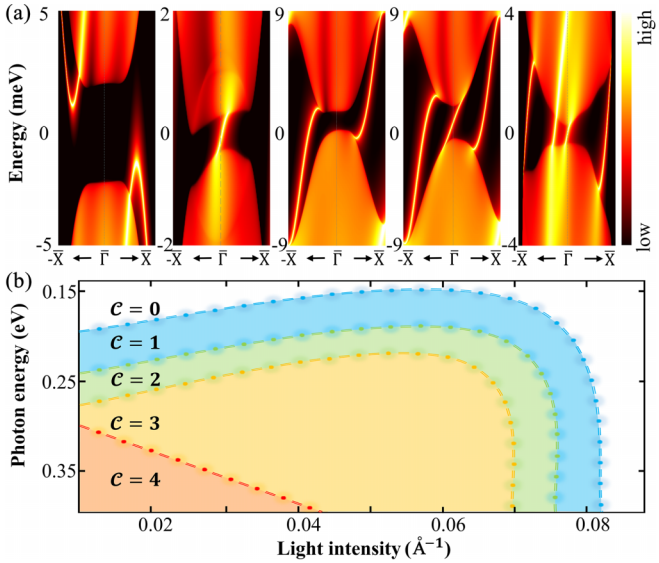

FIG. 4. Edge states and phase diagram of graphdiyne under the irradiation of CPL. (a) The edge states of graphdiyne along high-symmetry zigzag edge $-\overline{\mathrm{X}} \leftarrow \overline{\Gamma} \rightarrow \overline{\mathrm{X}}$ under the irradiation of CPL with different light intensity $eA/\hbar$ and photon energy $\hbar\omega$: The leftmost panel shows the trivial states of graphdiyne corresponding to $\mathcal{C}=0$ with $eA/\hbar = 0.06$ Å^{-1} and $\hbar\omega = 0.17$ eV; The second panel with $eA/\hbar = 0.05$ Å^{-1} and $\hbar\omega = 0.17$ eV exhibits the edge states with single chiral edge channels; The middle panel with $eA/\hbar = 0.07$ Å^{-1} and $\hbar\omega = 0.27$ eV corresponds to the nontrivial states of graphdiyne with $\mathcal{C}=2$; The edge states of graphdiyne with $\mathcal{C}=3$ are represented by the fourth panel ($eA/\hbar = 0.069$ Å^{-1} and $\hbar\omega = 0.27$ eV); The rightmost panel ($eA/\hbar = 0.02$ Å^{-1} and $\hbar\omega = 0.34$ eV) represents the edge states with four chiral edge channels for graphdiyne. (b) The Chern number phase diagram of graphdiyne under the irradiation of CPL as a function of light intensity and photon energy.

intensity and photon energy will suppress the high-Chern-number QAH states and lead to the decrease of Chern number rather than further increase it. This can serve as a useful guide for probing this topological state.

IV. SUMMARY

In summary, we propose a dynamic approach for achieving high-Chern-number QAH phases in periodically driven 2D HOTIs irradiated by CPL. To elucidate this, we focus on two representative types of 2D HOTIs whose bulk topology can be depicted by a quantized quadruple moment and the second Stiefel-Whitney number. We respectively choose the BBH model and the 2D graphdiyne to exhibit the photoinduced topological phase transition. This phase transition shows strong universality, i.e., the high-Chern-number QAH phase is derived from the light-induced multiple band inversion collaborated by higher-order band topology. The Chern number is continuously tunable from one to four by changing the light intensity and photon energy. Moreover, first-priciples calculations for the realistic material graphdiyne will greatly favor the experimental verification and further potential applications. Intriguingly, the irradiation of CPL does not destroy the quantized quadruple moment Q_{xy} in periodically driven HOTIs, and thus, the discovery that CPL triggers a phase transition to high-Chern-number QAH insulators from HOTIs not only establishes a strategy for designing high-Chern-number QAH insulators, but also unveils a unique Floquet topological state harboring both high Chern numbers and higher-order topology. Our work provides a powerful approach to investigate exotic topological states in nonequilibrium cases.

ACKNOWLEDGEMENTS

This work was supported by the National Natural Science Foundation of China (NSFC, Grants No. 12222402, No. 92365101, No. 12074108, No. 12304191, and No. 12347101), the Chongqing Natural Science Foundation (Grants No. CSTB2023NSCQ-JQX0024 and No. CSTB2022NSCQ-MSX0568), the Natural Science Basic Research Program of Shaanxi (Grant No. 2022JM-001), and the Fundamental Research Funds for the Central Universities (Grant No. 2023CDJXY-048).

[1] R. Yu, W. Zhang, H.-J. Zhang, S.-C. Zhang, X. Dai, and Z. Fang, Science **329**, 61 (2010).
[2] C.-Z. Chang, J. Zhang, X. Feng, J. Shen, Z. Zhang, M. Guo, K. Li, Y. Ou, P. Wei, L.-L. Wang, Z.-Q. Ji, Y. Feng, S. Ji, X. Chen, J. Jia, X. Dai, Z. Fang, S.-C. Zhang, K. He, Y. Wang *et al.*, Science **340**, 167 (2013).
[3] C.-Z. Chang, W. Zhao, D. Y. Kim, H. Zhang, B. A. Assaf, D. Heiman, S.-C. Zhang, C. Liu, M. H. W. Chan, and J. S. Moodera, Nat. Mater. **14**, 473 (2015).
[4] A. J. Bestwick, E. J. Fox, X. Kou, L. Pan, K. L. Wang, and D. Goldhaber-Gordon, Phys. Rev. Lett. **114**, 187201 (2015).
[5] C.-Z. Chang, C.-X. Liu, and A. H. MacDonald, Rev. Mod. Phys. **95**, 011002 (2023).
[6] D. J. Thouless, M. Kohmoto, M. P. Nightingale, and M. den Nijs, Phys. Rev. Lett. **49**, 405 (1982).
[7] Y. Deng, Y. Yu, Y. Song, J. Zhang, N. Z. Wang, Z. Sun, Y. Yi, Y. Z. Wu, S. Wu, J. Zhu, J. Wang, X. H. Chen, and Y. Zhang, Nature (London) **563**, 94 (2018).
[8] J. W. McIver, B. Schulte, F.-U. Stein, T. Matsuyama, G. Jotzu, G. Meier, and A. Cavalleri, Nat. Phys. **16**, 38 (2020).
[9] Y.-F. Zhao, R. Zhang, R. Mei, L.-J. Zhou, H. Yi, Y.-Q. Zhang, J. Yu, R. Xiao, K. Wang, N. Samarth, M. H. W. Chan, C.-X. Liu, and C.-Z. Chang, Nature (London) **588**, 419 (2020).
[10] H. Deng, Z. Chen, A. Wołoś, M. Konczykowski, K. Sobczak, J. Sitnicka, I. V. Fedorchenko, J. Borysiuk, T. Heider, Ł. Pluciński, K. Park, A. B. Georgescu, J. Cano, and L. Krusin-Elbaum, Nat. Phys. **17**, 36 (2021).
[11] T. Li, S. Jiang, B. Shen, Y. Zhang, L. Li, Z. Tao, T. Devakul, K. Watanabe, T. Taniguchi, L. Fu, J. Shan, and K. F. Mak, Nature (London) **600**, 641 (2021).

[12] P.-J. Guo, Z.-X. Liu, and Z.-Y. Lu, npg Comput. Mater. **9**, 70 (2023).

[13] J. Wang, B. Lian, H. Zhang, Y. Xu, and S.-C. Zhang, Phys. Rev. Lett. **111**, 136801 (2013).

[14] C. Fang, M. J. Gilbert, and B. A. Bernevig, Phys. Rev. Lett. **112**, 046801 (2014).

[15] H. Jiang, Z. Qiao, H. Liu, and Q. Niu, Phys. Rev. B **85**, 045445 (2012).

[16] K. Wang, J.-X. Dai, L. B. Shao, S. A. Yang, and Y. X. Zhao, Phys. Rev. B **105**, 085113 (2022).

[17] Z. Zhang, J.-Y. You, X.-Y. Ma, B. Gu, and G. Su, Phys. Rev. B **103**, 014410 (2021).

[18] W. Zhu, C. Song, H. Bai, L. Liao, and F. Pan, Phys. Rev. B **105**, 155122 (2022).

[19] J. Ge, Y. Liu, J. Li, H. Li, T. Luo, Y. Wu, Y. Xu, and J. Wang, Natl. Sci. Rev. **7**, 1280 (2020).

[20] Z. Li, Y. Han, and Z. Qiao, Phys. Rev. Lett. **129**, 036801 (2022).

[21] D. Wang, H. Wang, and H. Zhang, Phys. Rev. B **107**, 155114 (2023).

[22] T.-S. Xiong, J. Gong, and J.-H. An, Phys. Rev. B **93**, 184306 (2016).

[23] C. L. Kane and E. J. Mele, Phys. Rev. Lett. **95**, 226801 (2005).

[24] L. Fu and C. L. Kane, Phys. Rev. B **76**, 045302 (2007).

[25] B. A. Bernevig, T. L. Hughes, and S.-C. Zhang, Science **314**, 1757 (2006).

[26] L. Fu, C. L. Kane, and E. J. Mele, Phys. Rev. Lett. **98**, 106803 (2007).

[27] D. Hsieh, D. Qian, L. Wray, Y. Xia, Y. S. Hor, R. J. Cava, and M. Z. Hasan, Nature (London) **452**, 970 (2008).

[28] M. Z. Hasan and C. L. Kane, Rev. Mod. Phys. **82**, 3045 (2010).

[29] A. Bansil, H. Lin, and T. Das, Rev. Mod. Phys. **88**, 021004 (2016).

[30] W. A. Benalcazar, B. A. Bernevig, and T. L. Hughes, Phys. Rev. B **96**, 245115 (2017).

[31] W. A. Benalcazar, B. A. Bernevig, and T. L. Hughes, Science **357**, 61 (2017).

[32] F. Schindler, A. M. Cook, M. G. Vergniory, Z. Wang, S. S. P. Parkin, B. A. Bernevig, and T. Neupert, Sci. Adv. **4**, eaat0346 (2018).

[33] J. Langbehn, Y. Peng, L. Trifunovic, F. von Oppen, and P. W. Brouwer, Phys. Rev. Lett. **119**, 246401 (2017).

[34] Z. Song, Z. Fang, and C. Fang, Phys. Rev. Lett. **119**, 246402 (2017).

[35] E. Khalaf, Phys. Rev. B **97**, 205136 (2018).

[36] M. Geier, L. Trifunovic, M. Hoskam, and P. W. Brouwer, Phys. Rev. B **97**, 205135 (2018).

[37] R. Chen, C.-Z. Chen, J.-H. Gao, B. Zhou, and D.-H. Xu, Phys. Rev. Lett. **124**, 036803 (2020).

[38] F. Schindler, Z. Wang, M. G. Vergniory, A. M. Cook, A. Murani, S. Sengupta, A. Y. Kasumov, R. Deblock, S. Jeon, I. Drozdov, H. Bouchiat, S. Guéron, A. Yazdani, B. A. Bernevig, and T. Neupert, Nat. Phys. **14**, 918 (2018).

[39] R. Noguchi, M. Kobayashi, Z. Jiang, K. Kuroda, T. Takahashi, Z. Xu, D. Lee, M. Hirayama, M. Ochi, T. Shirasawa, P. Zhang, C. Lin, C. Bareille, S. Sakuragi, H. Tanaka, S. Kunisada, K. Kurokawa, K. Yaji, A. Harasawa, V. Kandyba *et al.*, Nat. Mater. **20**, 473 (2021).

[40] Y. Xu, Z. Song, Z. Wang, H. Weng, and X. Dai, Phys. Rev. Lett. **122**, 256402 (2019).

[41] X.-L. Sheng, C. Chen, H. Liu, Z. Chen, Z.-M. Yu, Y. X. Zhao, and S. A. Yang, Phys. Rev. Lett. **123**, 256402 (2019).

[42] F. Tang, H. C. Po, A. Vishwanath, and X. Wan, Nature (London) **566**, 486 (2019).

[43] F. Tang, H. C. Po, A. Vishwanath, and X. Wan, Nat. Phys. **15**, 470 (2019).

[44] Z. Wang, B. J. Wieder, J. Li, B. Yan, and B. A. Bernevig, Phys. Rev. Lett. **123**, 186401 (2019).

[45] M.-J. Gao, H. Wu, and J.-H. An, Phys. Rev. B **107**, 035128 (2023).

[46] B.-Q. Wang, H. Wu, and J.-H. An, Phys. Rev. B **104**, 205117 (2021).

[47] L. Trifunovic and P. W. Brouwer, Phys. Rev. X **9**, 011012 (2019).

[48] C.-A. Li, B. Fu, Z.-A. Hu, J. Li, and S.-Q. Shen, Phys. Rev. Lett. **125**, 166801 (2020).

[49] J. Ahn, D. Kim, Y. Kim, and B.-J. Yang, Phys. Rev. Lett. **121**, 106403 (2018).

[50] F. Zhan, J. Zeng, Z. Chen, X. Jin, J. Fan, T. Chen, and R. Wang, Nano Lett. **23**, 2166 (2023).

[51] E. Lee, R. Kim, J. Ahn, and B.-J. Yang, npj Quantum Mater. **5**, 1 (2020).

[52] N. H. Lindner, G. Refael, and V. Galitski, Nat. Phys. **7**, 490 (2011).

[53] Y. H. Wang, H. Steinberg, P. Jarillo-Herrero, and N. Gedik, Science **342**, 453 (2013).

[54] L. He, Z. Addison, J. Jin, E. J. Mele, S. G. Johnson, and B. Zhen, Nat. Commun. **10**, 4194 (2019).

[55] S. Ito, M. Schüler, M. Meierhofer, S. Schlauderer, J. Freudenstein, J. Reimann, D. Afanasiev, K. A. Kokh, O. E. Tereshchenko, J. Güdde, M. A. Sentef, U. Höfer, and R. Huber, Nature (London) **616**, 696 (2023).

[56] S. Zhou, C. Bao, B. Fan, H. Zhou, Q. Gao, H. Zhong, T. Lin, H. Liu, P. Yu, P. Tang, S. Meng, W. Duan, and S. Zhou, Nature (London) **614**, 75 (2023).

[57] H. Dehghani, T. Oka, and A. Mitra, Phys. Rev. B **91**, 155422 (2015).

[58] M. S. Rudner, N. H. Lindner, E. Berg, and M. Levin, Phys. Rev. X **3**, 031005 (2013).

[59] T. Mikami, S. Kitamura, K. Yasuda, N. Tsuji, T. Oka, and H. Aoki, Phys. Rev. B **93**, 144307 (2016).

[60] A. Gómez-León and G. Platero, Phys. Rev. Lett. **110**, 200403 (2013).

[61] H. Hübener, M. A. Sentef, U. De Giovannini, A. F. Kemper, and A. Rubio, Nat. Commun. **8**, 13940 (2017).

[62] M. S. Rudner and N. H. Lindner, arXiv:2003.08252.

[63] See Supplemental Material at http://link.aps.org/supplemental/10.1103/PhysRevB.109.085148 for the detailed computational methods and the discussions based on the $k \cdot p$ Hamiltonian, which inlcudes Refs. [41,57,65,67–69,74,75].

[64] W. Wang, X. Lüu, and H. Xie, Chin. Phys. B **30**, 066701 (2021).

[65] C. Chen, X.-T. Zeng, Z. Chen, Y. X. Zhao, X.-L. Sheng, and S. A. Yang, Phys. Rev. Lett. **128**, 026405 (2022).

[66] G. Li, Y. Li, H. Liu, Y. Guo, Y. Li, and D. Zhu, Chem. Commun. **46**, 3256 (2010).

[67] P. Hohenberg and W. Kohn, Phys. Rev. **136**, B864 (1964).

[68] G. Kresse and J. Furthmüller, Phys. Rev. B **54**, 11169 (1996).

[69] J. P. Perdew, K. Burke, and M. Ernzerhof, Phys. Rev. Lett. **77**, 3865 (1996).
[70] Y. Zheng, Y. Chen, L. Lin, Y. Sun, H. Liu, Y. Li, Y. Du, and N. Tang, Appl. Phys. Lett. **111**, 033101 (2017).
[71] N. Narita, S. Nagai, S. Suzuki, and K. Nakao, Phys. Rev. B **58**, 11009 (1998).
[72] M. Long, L. Tang, D. Wang, Y. Li, and Z. Shuai, ACS Nano **5**, 2593 (2011).
[73] U. De Giovannini, H. Hübener, and A. Rubio, Nano Lett. **16**, 7993 (2016).
[74] Q. Wu, S. Zhang, H.-F. Song, M. Troyer, and A. A. Soluyanov, Comput. Phys. Commun. **224**, 405 (2018).
[75] W. Kohn and L. J. Sham, Phys. Rev. **140**, A1133 (1965).